Lawrence Berkeley Laboratory
UNIVERSITY OF CALIFORNIA

Materials & Chemical Sciences Division

Presented at the Materials Research Society Fall Meeting,
Boston, MA, November 28–December 3, 1988, and
to be published in the Proceedings

Ab initio Calculations of Ordered Intermetallic Phase Equilibria

M. Sluiter, D. de Fontaine, X.Q. Guo, R. Podloucky,
and A.J. Freeman

December 1988

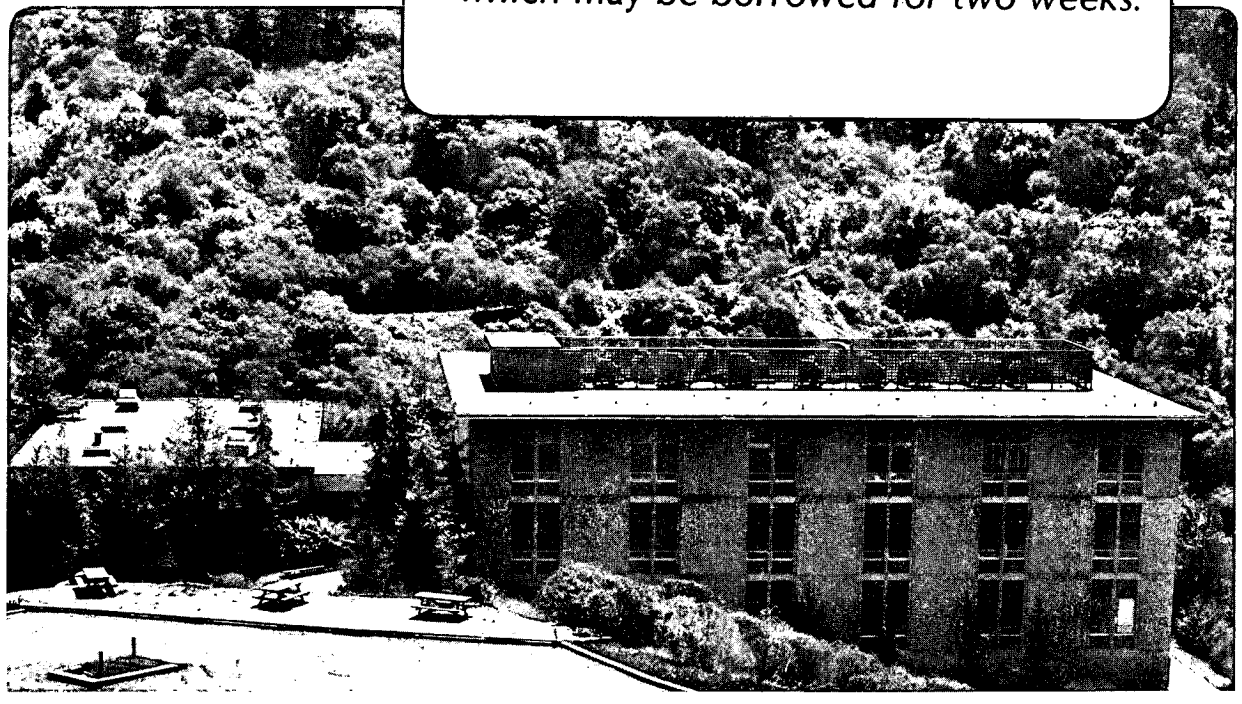

Prepared for the U.S. Department of Energy under Contract Number DE-AC03-76SF00098.

DISCLAIMER

AB INITIO CALCULATIONS OF ORDERED INTERMETALLIC PHASE EQUILIBRIA

M. SLUITER*, D. DE FONTAINE*, X.Q. GUO†, R. PODLOUCKY†§ AND A.J. FREEMAN†
*University of California, Dept. of Materials Science, Berkeley, CA 94720
†Northwestern University, Dept. of Physics, Evanston, Il 60207
§University of Vienna, Inst. for Physical Chemistry, A-1090 Vienna, Austria

ABSTRACT

General procedures for computing alloy phase equilibria from *ab initio* electronic structure calculations are reviewed and applied to the Al-Li phase diagram. Free energies were calculated by the cluster variation method (CVM) in the tetrahedron approximation for the fcc and bcc lattices and ordered superstructures. Input was provided by first principles FLAPW calculations. The computed phase diagram for both stable and metastable structures agrees remarkably well with the experimental one.

INTRODUCTION

The exciting possibility now exists of deriving phase diagrams virtually from first principles. There is value in determining even known phase diagrams by theoretical means alone since, once reasonable agreement has been achieved, correct thermodynamic functions are available and predictions can be made concerning equilibrium of stable and metastable phases, and properties can be predicted. Furthermore, a fundamental understanding of the underlying physics of the phase relations can be gained. The practical value of the undertaking is further enhanced when calculated binary phase equilibria are extended to include ternary, quaternary,...additions. It then becomes possible, in principle, to predict which elements are likely to stabilize which phases and *computer-aided alloy design*, or, in the words of Pettifor [1], "Quantum Engineering" becomes a distinct possibility.

Theory has made great strides in the last ten years or so in three quite distinct areas: (a) first principles total energy calculations of pure crystals and of simple stoichiometric compounds can now be performed very accurately thanks to density functional theory, (b) effective pair and cluster interactions (EPI, ECI) can now be calculated by the Gautier-Ducastelle [2] generalized perturbation method (GPM), having been implemented on tight-binding (TB) and KKR-CPA codes; and (c) a reliable statistical thermodynamical model has been developed to calculate realistic temperature-composition diagrams.

Let us dwell on this latter point. Until fairly recently, the standard free energy functions used in phase diagram calculations were the mean field, Gorsky-Bragg-Williams, regular of sub-regular solution models, method of concentration waves, or *zeroth approximation*; all of these methods are basically equivalent. In addition to being numerically inaccurate - transition temperatures can be off by 100% or more - these models predict the wrong phase diagram topology for fcc-based ordering systems and neglect short range order. These deficiencies can be remedied by use of the cluster variation method (CVM) [3], which was applied for the first time to phase diagram calculations by Van Baal [4] and by Kikuchi and one of the present authors [5]. A very complete treatment of the subject has been given recently by Finel [6]. The choice of free energy models is crucial to the subject matter of this symposium: important high-temperature alloy phases are ordered superstructures of the fcc lattice ($L1_2$, $D0_{22}$...), but ordering interactions are *frustrated* on this lattice. Hence, phase equilibrium in such systems, or metastable $L1_2$ in Al-Li, cannot be handled in the zeroth approximation, despite claims to the contrary.

The CVM requires, as input, interaction parameters which determine ordering or clustering reactions occurring in the alloy systems. These interactions must be defined carefully, then obtained numerically by means of electronic structure calculations. Thus, the statistical mechanical model dictates the type of quantum mechanical calculations to be performed. A

summary of the theoretical concepts will be give in the next two Sections. Application to the Al-Li system will be given in the final Section.

THE CVM SCHEME

Consider a binary alloy, with atoms A and B occupying N lattice sites. The operator σ_p at site p is defined as being +1 if p is occupied by A, -1 if occupied by B. Any one of 2^N *configurations* is defined by the set of all N operators σ_p. Such a description is neither feasible nor desirable. Instead, only a small set of *multisite correlation functions* ξ_α are defined by the ensemble average

$$\xi_\alpha = \langle \sigma_1 \sigma_2 \ldots \rangle_\alpha \tag{1}$$

where the σ operators specify the occupations of the points of the cluster α of n sites. It is shown [7] that the probability $\rho(\sigma)$ of finding the system in the configuration (σ) is given by

$$\rho(\sigma) = \rho_N^0 \left[1 + \sum_\alpha \sigma_\alpha \xi_\alpha \right] \tag{2}$$

where the sum is over all possible clusters of points in the crystal of N points, σ_α denoting the product of operators inside the bracket in Eq. (1). In Eq. (2), ρ_N^0 is the normalization 2^{-N}. The basic idea of the CVM is to truncate the summation in Eq. (2) after some maximal cluster, and to use such truncated expansions in both internal energy and configurational entropy expressions. Usually, only small clusters are manageable: tetrahedron, octahedron, cube... By comparison, the zeroth approximation truncates after a single lattice point.

The expectation value of the energy can be written as a weighted sum over all configurations

$$E = \sum_\sigma \rho(\sigma) E(\sigma) \tag{3}$$

where $E(\sigma)$ is the total energy of the specified configuration. Putting (2) into (3) yields

$$E = J_0 + \sum_\alpha J_\alpha \xi_\alpha \tag{4}$$

with

$$J_0 = \rho_N^0 \sum_\sigma E(\sigma) \tag{5}$$

and

$$J_\alpha = \rho_N^0 \sum_\sigma \sigma_\alpha E(\sigma) \tag{6}$$

The energy is thus expressed as a sum of *cluster interactions,* the J_α, weighted by corresponding correlations ξ_α. The case of pair interactions is of particular interest:

$$J(pq) = \frac{1}{2^2} \sum_{\sigma_p=\pm1} \sum_{\sigma_q=\pm1} \sigma_p \sigma_q \frac{1}{2^{N-2}} \sum_\sigma{}' E(\sigma) \tag{7}$$

where the last summation is over all configurations having specified σ at lattice points p and q. Equation (7) can be written

$$J(pq) = \frac{1}{4}(E_{AA} - E_{AB} - E_{BA} + E_{BB}) \qquad (8)$$

where E_{IJ} designates the energy of a pair cluster (I, J = A,B) embedded in a completely disordered average medium. These formulas can be extended to arbitrary clusters.

Often, the energy E is expressed only as a sum of *effective pair interaction* (EPI) of the type given by Eq. (8). It is important to note that these EPI's are *not* "pair potentials". Indeed, by Eqs. (7) and (8), we see that each E_{IJ} is in fact an energy for the whole crystal containing a certain type of pair (cluster). The EPI's (ECI) occur in the expression of the *ordering energy* (or Ising energy) and are typically two or three orders of magnitude smaller than the cohesive energy itself.

Despite the fact that ECI's are (small) differences of large numbers, methods have been developed to evaluate these from electronic structure calculations. Initially, these interactions were calculated in k-space by the GPM [2] or by the $S^{(2)}$ method of Györffy and Stocks [8], both methods relying on perturbing the coherent potential (CPA) medium. Later the GPM was formulated in direct space [9] and found to be equivalent to the embedded cluster method, the embedding medium being either the single-site CPA [10] or one obtained by configurational averaging [11,12]. The electronic structure calculations can be carried out either in Tight-Binding or KKR-CPA schemes.

The configurational entropy is obtained in the CVM approximation by expanding the exact expression $-k_B \Sigma \rho \ln \rho$ where k_B is Boltzmann's constant and the sum is over all possible configurations. An appropriate superposition approximation must be found which converges rapidly in the logarithms of "partial densities" [7] or cluster concentrations $x_\alpha(\sigma)$, i.e., the probability of finding cluster α having specified configuration σ at equilibrium. The required expression is

$$S = -k_B \sum_{\alpha} \gamma_\alpha \sum_{\sigma}^{\alpha} x_\alpha(\sigma) \ln x_\alpha(\sigma) \qquad (9)$$

where the first sum extends to all clusters up to the largest one retained in the chosen approximation and where the second summation is over the configurations of the specified cluster. The integers γ_α are so-called Kikuchi-Barker coefficients whose values are obtained by simple recursion formulas.

Each cluster (α) concentration can be expressed as a function of all multisite correlations ξ_β belonging to the cluster α and its subclusters (β), in a manner which exactly parallels that given in Eq. (2) for the whole crystal (considered as a supercluster). Since the x_α are linear functions of the correlations ξ , the free energy functional F = E - TS, with E given by Eq. (4) and S by Eq. (9), turns out to be an implicit function of the correlations:

$$F = F(\xi_1, \xi_2, ..., \xi_\alpha; T) \qquad (10)$$

The concentration dependence is implicit in the multisite correlations and explicit in the average "point" correlation $\xi_1 = 1 - 2c$, where c is the concentration of element B in the alloy AB. The equilibrium free energy is obtained by minimizing F in Eq. (10) with respect to the independent variables ξ at given temperature T and composition c, or in the grand canonical scheme, the difference of chemical potentials $\mu = \mu_A - \mu_B$.

The calculation is carried out at various T and c (or μ) for the various lattices and superstructures of interest, and phase diagrams are derived by constructing common tangents where appropriate. Not only are the equilibrium phase boundaries calculated, but, through the equilibrium correlations, states of LRO and SRO are determined as well. Moreover, Fourier transform methods also provide ordering and clustering spinodals [13] and SRO intensity [6,14,15].

Experience has shown that the CVM is a very reliable and general model which in most cases produces transition temperatures only a few percent off those determined exactly (as in the 2-dimensional Ising model) or by renormalization group or Monte Carlo techniques [6]. Bragg-Williams methods may suffice for curve fitting purposes, but the CVM (or Monte Carlo methods) must be used in the context of *ab initio* calculations.

ENERGY CALCULATIONS

For given phase φ, the CVM provides only the "Ising" or "ordering" contribution F_{mix} to the total free energy

$$F^{\varphi}_{tot} = F^{\varphi}_{lin} + F^{\varphi}_{mix} \tag{11}$$

where the term linear in concentration

$$F^{\varphi}_{lin} = (1-c)\ F^{\varphi}_{A} + c\ F^{\varphi}_{mix} \tag{12}$$

combines the free energies of pure elements A and B:

$$F^{\varphi}_{I} = E^{\varphi}_{I} - T S^{\varphi}_{I}\ ,\ (I = A \text{ or } B) \tag{13}$$

in which the cohesive energy E^{φ}_{I} and vibrational entropy S^{φ}_{I} are both considered to be practically temperature independent. It is essential to include the linear term if CVM free energies of phases based on different lattices need to be compared.

The parameters required for a complete free energy determination, for given structure or superstructure φ, are thus the following: cohesive energies of pure A, B and effective cluster interactions for each phase φ, for all clusters envisioned, and the configuration-independent energy J^{φ}_{0} which appears in Eq. (4) along with the ECI, J^{φ}_{α}. Both J_0 and J_α (all α) are generally concentration dependent but may be regarded as temperature independent. The vibrational entropy may be estimated by empirical means.

The *pure element* cohesive energies can be obtained quite accurately by first principles electronic structure calculations. The *alloy* energies $J^{\varphi}_{0}(c)$, $J^{\varphi}_{\alpha}(c)$, may be obtained by either of two rather different procedures: the starting point for one is the fully disordered state, that for the other are the fully ordered states.

In the first method, the energy of the completely disordered solid solution is calculated either by the coherent potential approximation (CPA)[16,17] or by configurational averaging [11,12]. The ECI (EPI) are calculated by the generalized perturbation method (GPM)[2], or by the embedded cluster method (ECM)[10] or by direct configurational averaging (DCA)[11,12]. In the first two cases, the average medium is the single site CPA, in the third it is a random solid solution. All of these electronic structure calculations may be performed at absolute zero of temperature. Thus, a very convenient decoupling of energy and configurational entropy calculations is achieved: all parameters required as input to the CVM free energies are obtained by 0 K calculations, the temperature dependence comes in through the correlation functions ξ by free energy minimization at various values of T. Prototype phase diagrams were calculated in this way for hypothetical fcc-based systems by Turchi *et al.*[18] , for bcc systems by Sigli and Sanchez [19] and by the present authors for the combined fcc-bcc-liquid Ti-Rh system [20].

THE Al-Li SYSTEM

In the second method, the so-called Connolly and Willliams method [21], this decoupling is realized as well. Here, for each lattice, one performs accurate *ab initio* total energy calculations of as many stoichiometric ordered superstructures (including pure element) as there are unknown ECI's required by the CVM approximation chosen. For these perfectly ordered structures, the correlations ξ are known so that the linear system (4) can be inverted to yield the desired sets of J^{φ}_{0} and J^{φ}_{α}. This procedure has been used successfully by Zunger and co-workers [22,23] and by Terakura and co-workers [24,25].

Table I. FLAPW results for fcc and bcc based structures. The cohesive energy E_{coh} is defined as the difference of the energy of one mole of atoms in the solid state and the energy of one mole of atoms in the infinitely diluted gas state (infinite interatomic distances). The equilibrium molar volume and the bulk modulus are represented by V and B, respectively.

structure	E_{coh} kJ/mole	V_0 cm ^{3}/mole	B GPa
Al - fcc	387.164	9.5533	82.198
Al_3Li - $L1_2$	342.297	9.4518	70.305
AlLi - $L1_0$	288.765	9.2805	50.409
$AlLi_3$ - $L1_2$	225.911	9.7403	28.370
Li - fcc	164.108	11.4031	13.642
Al - bcc	381.125	9.6068	84.184
$Al_3Li - DO_3$	329.299	9.6518	55.844
AlLi - B2	289.027	8.8921	42.091
AlLi - B32	297.167	9.2148	57.750
$AlLi_3 - DO_3$	230.244	9.6829	29.640
Li - bcc	163.452	11.4387	15.246

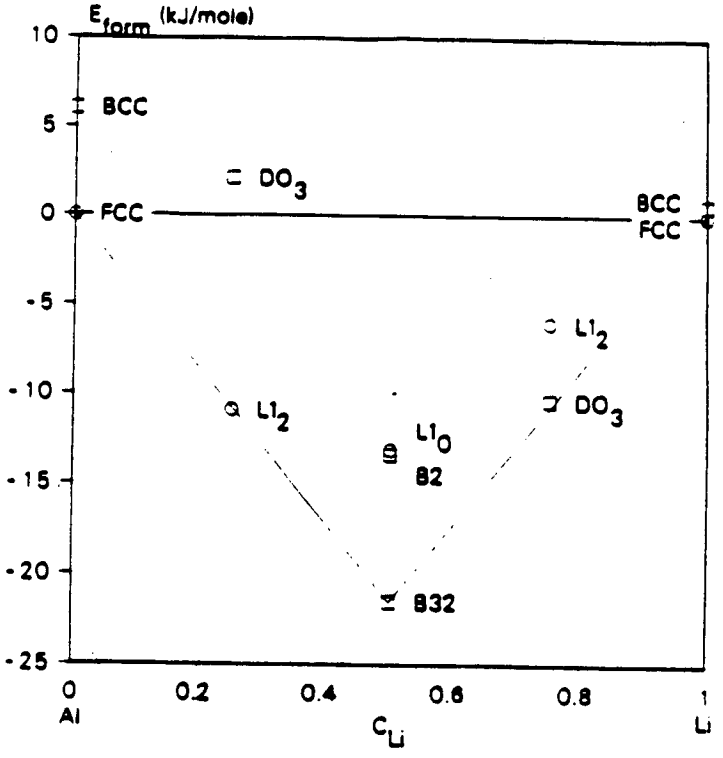

Figure 1. The formation energy E_{form} as a function of composition. This plot shows the phase equilibria at 0 K. The circles and squares correspond to structures based on the fcc and bcc lattice, respectively. The Al_3Li – $L1_2$ phase is just below the (solid) line connecting the Al-fcc and B32 phases, an indication that the $L1_2$ phase is just stable at 0 K. The AlL_3 – $L1_2$ phase is far above the (dashed) line connecting the Li-fcc and B32 phases, indicating that this $L1_2$ phase is not stable at 0 K (nor at any other temperature).

The present authors have used this method for calculating phase equilibria in the Al-Li system [29]. The *ab initio* total energy computations were performed by the FLAPW method. In the Al-Li, as in the Ti-Rh system, equilibrium is conditioned by the competition between fcc and bcc lattices and their respective superstructures. The structures chosen are listed in Table I. This set suffices since the CVM calculations were performed in the tetrahedron approximation. For fcc, the nearest-neighbor tetrahedron comprises 4 subclusters; the point, the (first) pair, the triangle and the tetrahedron itself. An additional calculation is required to obtain the J_0^{fcc} term, so five total energy values are necessary. For bcc, the tetrahedron includes also the second neighbor pair so that six energy calculations are required. The FLAPW computations were

performed for each structure for different values of the (cubic) lattice parameter. The energy values were fitted to a parabola, the minimum of which determined the equilibrium lattice parameter at 0 K. The curvature at the minimum yielded the bulk modulus β. Table I gives the calculated equilibrium cohesive energies, molar volume and bulk modulus. Table II compares calculated values with those determined experimentally . Theoretical and experimental structural energies and formation energies are also compared.

The structures selected for energy calculations were *all* the *fcc* and *bcc* superstructures stabilized by predominantly nearest neighbor ordering interactions. Thus, there was no *a priori* bias in the selection. It is instructive to plot the "formation" energies of these structures as a function of stoichiometry. This was done in Fig. 1 which is thus the graphical representation of Table I. Here, the formation energy is defined as the total energy of the structure of interest minus that of the pure elements *in the fcc phase*. Thus, in Fig. 1, fcc Al and Li are on a horizontal straight line at level zero. All fcc-related structures are denoted by circles, the bcc-related structures by squares. The ground states of both Al and Li are predicted to be fcc, although bcc Li has energy only slightly higher than fcc. Actually, Li does transform to a close-packed structure below about 78 K [26], but becomes bcc at higher temperature because of vibrational entropy contributions to the free energy. A remarkable feature of the calculation is that the B32 structure is predicted to be much more stable that the B2 or $L1_0$ at c = 1/2 stoichiometry. Indeed, the so called δ phase at the center of the Al-Li diagram has the B32 structure. The experimentally determined phase diagram is shown in Fig. 2 [27]. At c = 1/4, an $L1_2$ superstructure is predicted to be just barely stable with respect to a mixture of fcc and B32 phases. At higher temperatures, the $L1_2$ is expected to become metastable with respect to that mixture, as is observed experimentally [28]. In the literature, this phase is denoted by the symbol δ'; we prefer to call it α', since it is a superstructure of fcc, which is designated as α in Al-Li phase diagrams. At c = 3/4, it is a bcc superstructure which becomes stable, the DO_3. In reality, "interloper" line compounds are observed on that side of the phase diagram.

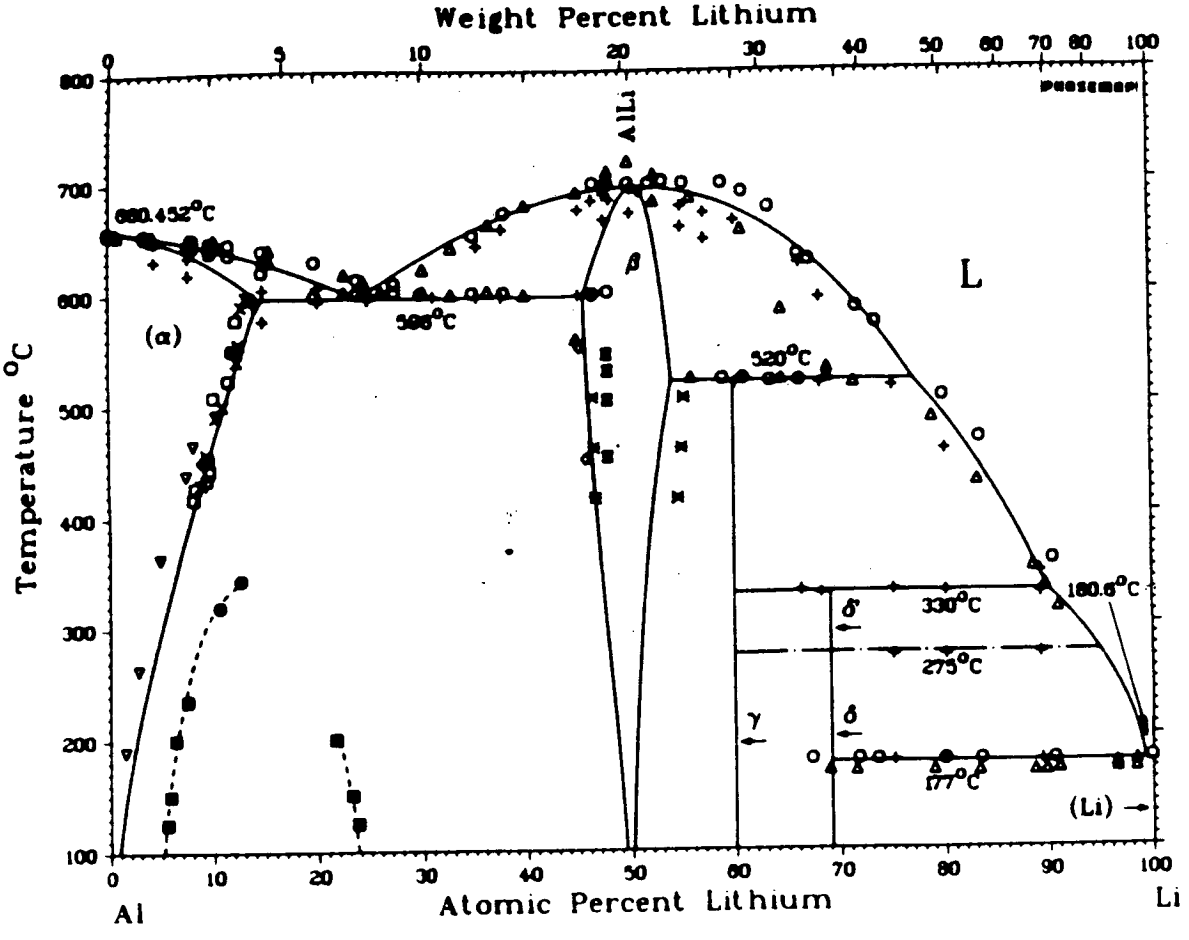

Figure 2. The Al-Li phase diagram according to an assessment by McAlister [27].

The remarkable prediction of correct ground states augures well for a complete phase diagram calculation. The procedure followed is described in detail in the original paper [29], and can be summarized as follows: As mentioned, the total energy of each structure φ at 0 K may be expressed as a quadratic in volume V

$$E^{\varphi}(V) = W_0^{\varphi} + W_1^{\varphi} V + W_2^{\varphi} V^2 \qquad (14)$$

the coefficients W of which may be evaluated numerically from the FLAPW results. Hence, for each *lattice* (fcc or bcc) and its family of superstructures, the total energy may be written explicitly in matrix form as

$$\mathbf{E} = \mathfrak{W}\, \mathbf{V} \qquad (15)$$

where **E** is a vector containing the n structure energies E^{φ}, $\mathfrak{W}$ is an 3xn matrix of W_i^{φ} (i = 1,2,3) and **V** is the vector [1, V, V^2]. The Sanchez equation [7] may also be written in matrix form (with $1 = \xi_0$)

$$\mathbf{E} = \mathfrak{X}\, \mathbf{J} \qquad (16)$$

where $\mathfrak{X}$ is the (square) matrix of stoichiometric correlations ξ_{α} and **J** is the vector of ECI's for the *lattice* considered. According to the Connolly and Williams prescription [21], Eq. (15) can be inverted to yield the required ECI's:

$$\mathbf{J} = \mathfrak{X}^{-1}\, \mathbf{E} = \mathfrak{X}^{-1}\, \mathfrak{W}\, \mathbf{V} \qquad (17)$$

where Eq. (15) has been used. It is now possible to write down explicit expressions for the ECI's as a function of volume

$$J_{\alpha}(V) = J_{\alpha}^{(0)} + J_{\alpha}^{(1)} V + J_{\alpha}^{(2)} V^2 \qquad (18)$$

in which the coefficients $J_{\alpha}^{(k)}$ (k = 0, 1, 2) are elements of the matrix $\mathfrak{X}^{-1}\, \mathfrak{W}$. There are as many equations (18) as there are clusters retained in the CVM energy expression, times the number of lattices considered.

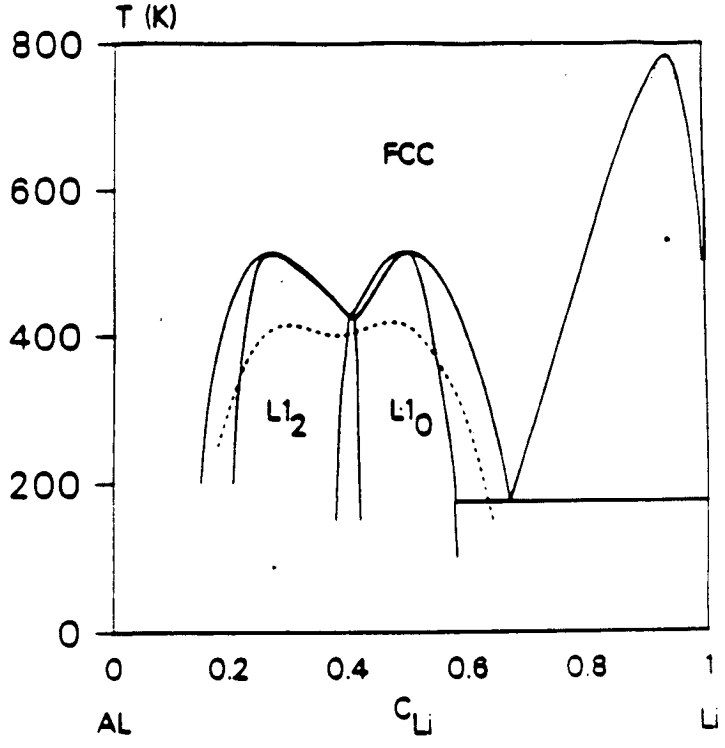

Figure 3. The Al-Li phase diagram calculated with only fcc based structures taken into account. Relaxation effects, as described in section VI.2.4, have not been included. The dotted line represents the [000] phase separation spinodal and the dashed curve indicates the [100] ordering spinodal.

When expressions (18) are introduced into Eq. (4), the CVM free energy functional becomes volume dependent, which means that the equilibrium free energy must be obtained by minimization with respect to both correlation variables ξ_α and volume V. The minimization is commonly carried out by Newton-Raphson iteration. Note that the Hessian of the successive linear systems may become singular in which case the thermodynamic phase under consideration would become unstable with respect to configurational, mechanical or mixed modes [29]. At each temperature and concentration the minimization thus produces free energies of ordered and disordered phases along with equilibrium values of all correlations ξ (hence LRO and SRO) and of volume V. The common tangent construction determines stable and metastable phase boundaries.

If only fcc-based equilibria are considered, the phase diagram of Fig. 3 is produced. Both $L1_2$ (metastable α') and $L1_0$ phase regions are obtained. The large miscibility gap on the Li side is caused by elastic effects. Note that absolute values of ordering temperatures are calculated since absolute values of ECI J_α are determined by Eq. (17) at equilibrium values. The dashed line is the calculated *ordering spinodal* [13] for <100> ordering waves. Below this limit of stability, Cu-Au-type ordering should take place homogeneously. All transitions are first order.

The bcc-only phase diagram is shown in Fig. 4. Note that B32 disordering takes place at a very high temperature. A DO_3 phase is expected at high Li content. At low Li content, the metastable bcc solid solution should spinodally decompose below the indicated dotted line.

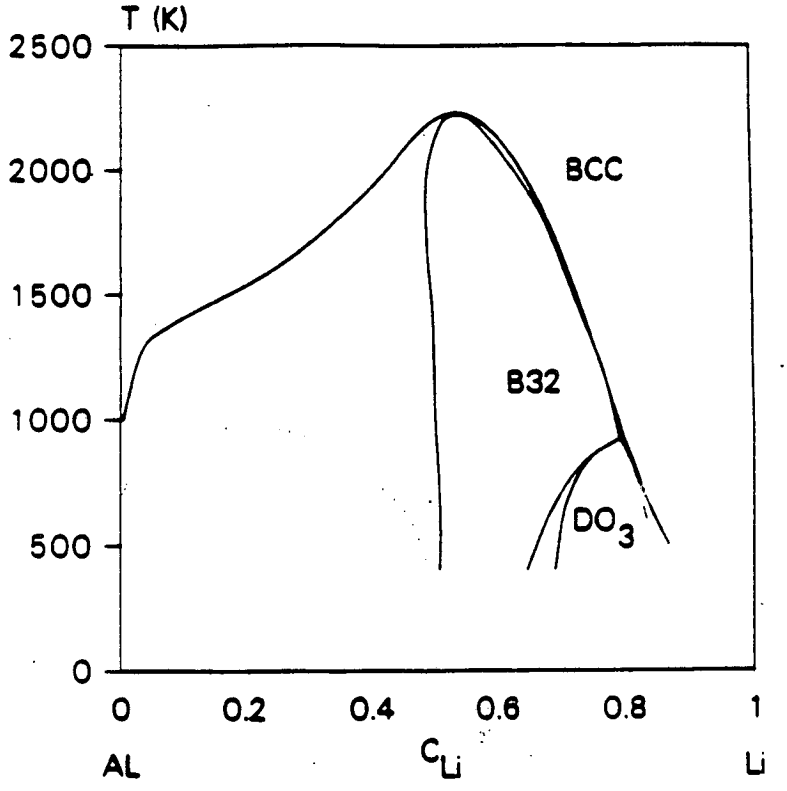

Figure 4. The bcc Al-Li phase diagram without relaxation. The dotted line indicates the metastable miscibility gap in the disordered bcc solid solution.

When families of both fcc- and bcc- based free energy curves are combined, the phase diagram of Fig. 5 is obtained. Dashed lines refer to the fcc-only equilibria now seen to relate to metastable phases. It is imperative to recognize that the diagram of Fig. 5 results from a pure *first principles calculation*: the only input parameters were the atomic number $Z_{Li} = 3$ and $Z_{Al} = 13$. Although resemblance with the experimental diagram (Fig. 2) may not be immediately apparent, certain basic features are predicted correctly: a wide fcc solid solution field on the Al side, very low solubility on the Li side, a central B32 phase persisting to very high temperatures, and $L1_2$ (α') Al_3Li metastable phase with rather low disordering temperature (the calculated 500 K is a bit low, α' actually persists to at least 400 °C). The predicted metastable $L1_0$ has not been observed experimentally due to the impossibility of quenching an fcc phase at such high Li concentrations, only fcc + B32 two-phase equilibrium being accessible.

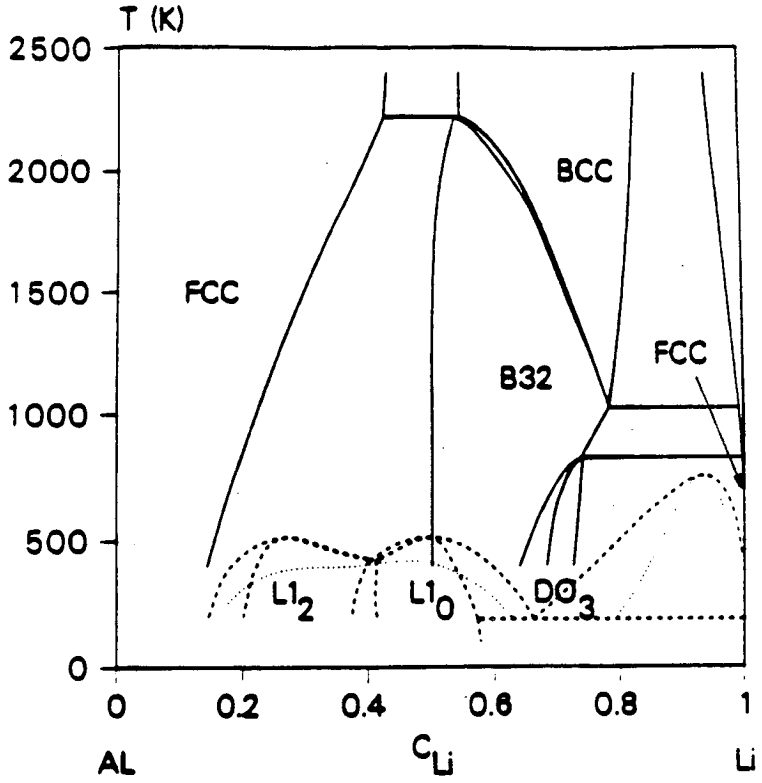

Figure 5. The solid-state part of the Al-Li phase diagram. Both fcc and bcc based phases have been included. The fcc based ordered phases have been repressed because of the greater stability of the bcc based structures. The metastable fcc-based equilibria are indicated with dashed lines. The [100] fcc ordering spinodal is denoted with a dotted line. Note that at this stage no experimental data have entered the computation

Clearly, two additional features are missing from the phase diagram of Fig. 5: the solid-liquid equilibria and the fcc→bcc allotropic phase transformation on the Li side. To incorporate these features, some empirical parameters must be introduced. We chose to represent the liquid free energy curve by a regular solution model with parameters fixed by the melting temperatures of pure fcc Al, bcc Li and B32 congruent melting. Also, a vibrational entropy correction was introduced in such a way as to produce the close-packed to bcc transition of pure Li at the observed temperature. The chosen parameters are given elsewhere [29].

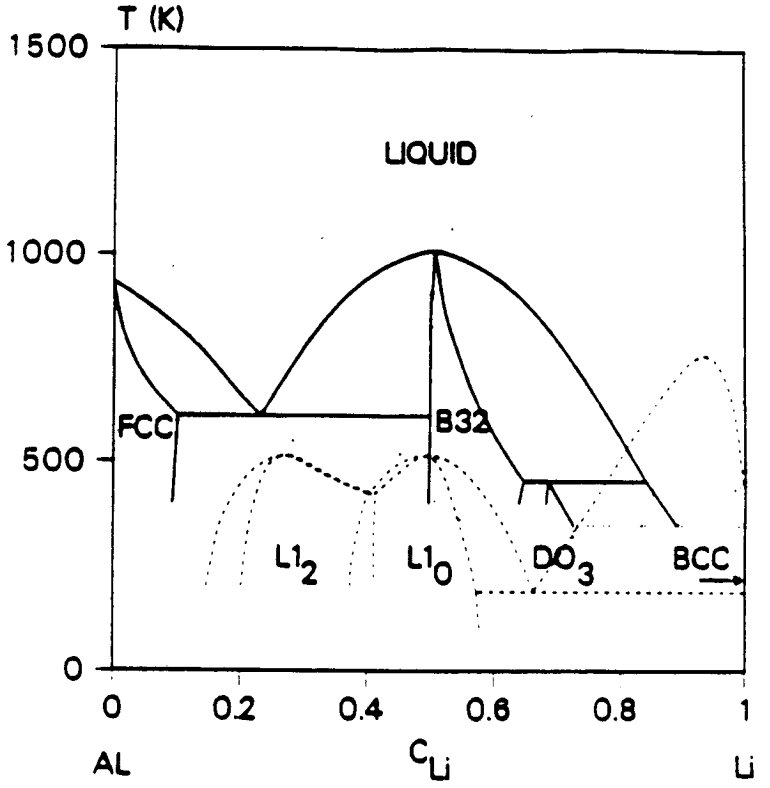

Figure 6. As figure VI.8 but now including the empirical vibrational-entropy difference between fcc and bcc based phases.

The complete diagram constructed by combining the first principles calculation (leading to Fig. 5) and the empirical corrections just described is shown in Fig. 6. Now the agreement with the diagram of Fig. 2 is indeed striking. Eutectics are correctly predicted to exist at both Al and Li sides and the B32 is shown to melt congruently. The calculated eutectic temperatures are a bit low but that is caused by our choice of a rather simplistic liquid free energy model. The "interloper" phases Al_2Li_3 and Al_4Li_9, not being superstructures of either fcc or bcc, do not appear in this computation but the rather similar DO_3 may be regarded as representing the actual intermetallics; the narrow-range DO_3 phase is predicted to form by peritectic reaction, as do the actual "incoherent" intermetallics.

DISCUSSION

If the qualitative agreement is good between experimental and theoretical phase diagrams, thermodynamic values derived from the calculation also may be expected to agree closely with experimental ones. Tables II and III indicate that this is indeed the case.

In Table II theoretical (FLAPW) and experimental values are compared for cohesive energies, equilibrium volume, bulk modulus, structural and formation energies. The cohesive energies of fcc-Al and bcc-Li agree remarkably well with sublimation energies (extrapolated to 0 K). It is then reasonable to assume that calculated cohesive energies of bcc-Al and fcc-Li are also accurate, although experimental values are note available, of course. The calculated and measured equilibrium volumes (V_0) also are in excellent agreement, even for the metastable Al_3Li ($\alpha' - L1_2$) phase. Bulk moduli (β) also agree well, particularly when the experimental value is corrected to 0 K. Cohesive energy differences between fcc and bcc pure Al and Li cannot be measured but can be estimated from the experimental phase diagram in an indirect way [30]. Here, some discrepancies arise; but as pointed out by Miodownik [31], the "experimental" values may well be rather inaccurate. That is surely the case for Li since the ground state is a close-packed structure, hence $\Delta E^{fcc\text{-}bcc}$ must be positive, not negative as deduced from the phase diagrams [32]. The calculated formation energy of B32 falls between experimental ones, and is in fact closer to one of those values than are the experimental ones to one another.

Table II. A comparison of various physical properties computed with the FLAPW method (this work) with available experimental data. Units are kJ/mole for the structural-energy difference $\Delta E^{fcc-bcc}$ and for the energies of sublimation, cohesion and formation E_{sbl}, E_{coh}, E_{form}, respectively, and cm^3/mole and GPa for the equilibrium volume V_0 and the Bulk modulus B. The bulk moduli are followed by the temperature in brackets. For the structural energies and the formation energy no experimental data was available, instead a comparison is made with results obtained from phase-diagram fitting (listed under "fitting"). References pertaining to experimental data are given elsewhere [29].

property	phase	FLAPW	experiment
E_{coh} :: E_{sblm}	Al-fcc	387.2	322.4
	Li-bcc	164.1	161.1
V_0 (298K)	Al-fcc	9.5533	9.7861
	B32	9.2148	9.3849
	Li-bcc	11.4387	12.391
	Li-fcc	11.4031	12.288
	Al_3Li-$L1_2$	9.4518	9.439
B	Al-fcc	82.2 (0 K)	83.3 (0 K)
			75.2 (295 K)
			76.6 (295 K)
			77.3 (295 K)
	Al_3Li-$L1_2$	70.3 (0 K)	66. (295 K)
	Li-bcc	15.2 (0 K)	12. (295 K)
Property	phase	FLAPW	fitting
$\Delta E^{fcc-bcc}$	Al-bcc	6.039	10.086
	Li-bcc	0.656	-1.214
E_{form}	B32	-21.531	-15.633
			-23.685

All theoretical values reported in Table II are deduced from FLAPW calculations. Those given in Table III required CVM calculations, in addition, and are therefore more critical test of the overall model. As examples, we compare theoretical (this work) and experimental values of lattice parameter variations as a function of concentration for fcc-Al and for B32.

Once again, the agreement is very good. That does not seem to be the case for the parameter δ, the misfit, at equilibrium, between Al and Al_3Li. Agreement is fairly good also for the variation of bulk modulus (in the fcc Al-rich solid solution) as a function of Li content. The bulk modulus is seen to decrease with Li additions. It has been reported that Young's modulus increases with Li contents [33], which means that Poisson's ratio must behave anomalously at high Li concentration.

Table III. A comparison of theoretical CVM predictions and experimental measurements. The change of the lattice parameter per atomic percent lithium ($\partial a/\partial c_{Li}$) in nm units in the aluminum rich fcc solid solution (fcc-Al) and the B32 phase and the change of the bulk modulus per atomic percent lithium ($\partial B/\partial c_{Li}$) in GPa units in the fcc-Al phase from CVM computations (this work) and as reported in the literature. The misfit parameter δ, in percent, given by eq. (VI.16), between the fcc-Al phase and the Al_3Li-$L1_2$ precipitates, from lattice parameters computed with the CVM (no relaxation) at 300 and 500 K, and as experimentally observed. References pertaining to the experimental data are given elsewhere [29].

property	phase	this work	experiment
$\partial a/\partial c_{Li}$	fcc-Al	-.000051	-.000029 -.000044 -.000069
$\partial a/\partial c_{Li}$	B32	-.00022	-.00025 -.00034
δ (300K)	fcc-Al/Al_3Li-$L1_2$	-.28	-.08 -.09
δ (500K)	fcc-Al/Al_3Li-$L1_2$	-.19	
$\partial B/\partial c_{Li}$	fcc-Al	-.48	-.576

Only portions of the two-phase region $\alpha + \alpha'$ have been determined experimentally. The calculation, however, clearly shows the full metastable equilibrium, including the $L1_2 - L1_0$ phase boundaries. Clearly, the theoretically determined $\alpha + \alpha'$ region is too narrow and too far towards high Li-content. But let us recall, once again, that the present calculation makes use of the two atomic numbers Z_{Al} and Z_{Li} as only input parameters. Previously calculated phase boundaries were obtained by fitting to the experimental points. In the calculation of Sigli and Sanchez [34], a low-lying miscibility gap was found, whereas the present calculation does not predict such a feature. It is likely, however, that this metastable gap is a feature of the particular fitting procedure used [34]. Khachaturyan et al. [35] also obtained portions of $\alpha + \alpha'$ phase boundaries by fitting to a "concentration wave" free energy, which is in fact the Bragg-Williams model under a different name. Since two adjustable parameters were used, it is not surprizing that the fitted curve passed close to the experimental points. Khachaturyan et al. failed to show the upper portion of their calculated phase boundaries; actually, their model would predict that both $L1_2$ and $L1_0$ ordered regions merge into a double second-order critical point at $c = 0.5$, which is clearly unacceptable. It is probable that the present CVM calculation could be improved by including second neighbor EPI's in the fcc calculation. The second EPI may have appreciable magnitude as the (sp) wave functions of both Al and Li are expected to overlap several neighbors.

Additionally, the calculations presented here provide a fundamental understanding of the physics underlying the phase diagram. Basically, the Al-Li thermodynamics can be viewed as resulting from a bcc-fcc competition: fcc clearly dominates on the Al side, with the fcc solid solution and the metastable $L1_2$ fcc superstructure, whereas bcc dominates on the Li side, with the $D0_3$ and very narrow bcc Li terminal phase. Actually, Li should prefer fcc, but the cohesive energy of bcc Li is so close to fcc that bcc dominates above room temperature due to vibrational entropy effects. The case of B32 is intriguing. In many binaries which have fcc terminal solid

solutions a bcc superstructure is stabilized at central compositions. This is undoubtedly because ordering is preferred on a bcc lattice compared to fcc ordering, such as $L1_0$, which is *frustrated.* Hence for given nearest neighbor EPI, the ordering transition temperature for bcc ordering will be much higher than that for fcc ordering, as observed when comparing Figs. 3 and 4. In other words, the energy lost in "promoting" the bcc over the fcc lattice is more than recovered by bcc rather than fcc ordering. That, in this system, B32 is preferred over B2 is undoubtedly due to the longer range effective interactions expected in (sp) bonding.

CONCLUSIONS

It was shown by an example that *ab initio* phase diagram computations are becoming feasible thanks to the way significant progress realized recently in combining both quantum and statistical mechanical calculations in a highly ingrated, accurate and reliable manner. It is hoped that, in the near future, it may be possible to accomplish the following task quite generally: given basic information for pure A and B (and C), such as electronic structure,bulk moduli, melting and allotropic transition temperatures, construct the corresponding A-B (or A-B-C) phase diagram with no additional "alloy" data. In other words, what is being developed is an interpolating scheme for predicting stable and metastable alloy phase equilibria using, as input, only pure element parameters. Such is the first step towards a *first principles thermodynamics of materials.*

ACKNOWLEDGEMENTS

Research at the University of California was funded by the Air Force Wright Aeronautics Lab. administered through Los Alamos National Laboratory. Research at Northwestern University was supported by an NFS (grant no. DMR 85-18607 and by a grant from its Division of Advanced Computing at the Pittsburgh Supercomputer Center) and the Air Force Office of Scientific Research (grant no. 85-0358). R.P. acknowledges the support of the Austrian Ministry of Science (project no. 49.554/3-24/87). Work on the Ti-Rh system was originally supported by a grant from the Lawrence Livermore National Lab. and the Office of Energy Research. Materials Sciences Division, US Department of Energy, under contract DE-ACO3-76SF 00098.

REFERENCES

1. D. Pettifor, New Scientist 110, No. 1510, 48-52 (1986).
2. F. Ducastelle and F. Gautier, J. Phys. F: Met. Phys. 6, 2039 (1976).
3. R. Kikuchi, Phys. Rev. 81, 988 (1951)
4. C.M. van Baal, Physica (Utrecht) 64, 571 (1973).
5. D. de Fontaine and R. Kikuchi, in Applications of Phase Diagrams in Metallurgy and Ceramics, edited by G.C. Carter, NBS Special Publication: 496, Gaithersburg, Md, (1978), p. 999.
6. A. Finel, These de Doctorat d'Etat, University of Paris VI (1987).
7. J.M. Sanchez, F. Ducastelle and D. Gratias, Physica (Utrecht) 128A, 334 (1984).
8. B. Györffy and G.M. Stocks. Phys. Rev. Lett. 50, 374 (1983).
9. P. Turchi, These Doctorat d'Etat, University of Paris VI, 1984.
10. A. Gonis and J.W. Garland, Phys. Rev. B 16, 2424 (1977).
11. A.Berera, H. Dreyssé, L.T. Wille, and D. de Fontaine, J. Phys. F: Met. Phys. 18, L49 (1988).
12. H. Dreyssé, A. Berera, L.T. Wille and D. de Fontaine, Phys. Rev. B (in press).
13. D. de Fontaine, Solid State Physics, edited by H. Ehrenreich, F. Seitz and D. Turnbull, Vol. 34, pp. 73-294, Acad. Press, N.Y. (1979).
14. J.M. Sanchez, Physica (Utrecht) 111A, 200 (1982).
15. T. Mohri, J.M. Sanchez, and D. de Fontaine, Acta Mettall. 33, 1463 (1985).
16. B. Velicky, S. Kirkpatrick, and H. Ehrenreich, Phys. Rev. 175, 747 (1968).
17. J.S. Faulkner, Prog. Mater. Sci. 27, 1 (1982).
18. P. Turchi, M. Sluiter, and D. de Fontaine, Phys. Rev. B 36, 3161 (1987).

19. C. Sigli and J.M. Sanchez, Acta Metall. 34, 1021 (1986); ibid. 36, 367 (1988).
20. M. Sluiter, P. Turchi, Z. Fu, and D. de Fontaine, Phys. Rev. Lett. 60, 716 (1988).
21. J.W.D. Connolly and A.R. Williams, Phys. Rev. B 27, 5169 (1983).
22. A. Zunger, S.-H. Wei, A.A. Mbaye, and L.G. Ferreira, Acta Metall. 36, 2239 (1988).
23. L.G. Ferriera, A.A. Mbaye, and A. Zunger, Phys. Rev. B 35, 6475 (1987); A.A. Mbaye, L.G. Ferreira, and A. Zunger, Phys. Rev. Lett. 58, 49 (1987).
24. K. Terakura, T. Oguchi, T. Mohri, and K. Watanabe, Phys. Rev. B 35, 2169 (1987).
25. T. Mohri, K. Terakura, T. Oguchi, and K. Watanabe, Acta Metall. 36, 547 (1988).
26. H.G. Smith, Phys. Rev. Lett. 58, 1228 (1987).
27. A.J. McAlister, Bull. Alloy. Phase Diag. 3, 177 (1982).
28. B. Noble, and G.E. Thompson, Metal Sci. J., 5, 114 (1971); D.B. Williams, and J.W. Edington, Metal Sci. J., 9, 529 (1975); S. Ceresara, S. Cocco, G. Fagherazzi, and L. Schiffini, Phil. Mag., 35, 97 (1977); S. Cocco, G. Fagherazzi, and L. Schiffini, J. Appl. Cryst., 10, 325 (1977); F. Livet, and D. Bloch, Scripta Met., 10, 1147 (1985); M. Kraitchman, Thesis University of California Berkeley (1989).
29. M. Sluiter, D. de Fontaine, X.Q. Guo, R. Podloucky and A.J. Freeman. (Submitted for publication in Phys. Rev. B).
30. L. Kaufman and H. Bernstein, in Computer Calculation of Phase Diagrams, Acad. Press, NY (1970).
31. A.P.Miodownik, in Computer Modeling of Phase Diagrams, edited by L.H. Bennett, AIME, Warrendale PA, (1986), p. 253.
32. M.L. Saboungi and C.C. Hsu, Calphad 1, 237 (1977).
33. B. Noble, S.J. Harris, and K. Dinsdale, J. Mat. Sci. 17, 461 (1982); W. Mueller, E. Bubeck, and V. Gerold, Proc. 3rd Int. Conf. Aluminum-Lithium Alloys, edited by C. Baker, P.J. Gregson, S.J. Harris and C.J. Peel, TMS-AIME, London (1986), pp. 435; E. Agyekum, W. Kuch, E.A. Starke Jr., S.C. Jha, and T.H. Sanders Jr., ibid, pp.448.
34. C. Sigli and J.M. Sanchez, Acta Metall. 34, 1021 (1986); C. Sigli, Ph.D. Thesis, Columbia University, New York (1987).
35. A.G. Khachaturyan, T.F. Lindsay and J.W. Morris, Jr., Met. Trans. 19A, 249 (1988).

LAWRENCE BERKELEY LABORATORY
TECHNICAL INFORMATION DEPARTMENT
1 CYCLOTRON ROAD
BERKELEY, CALIFORNIA 94720